ELSEVIER

Physica E 6 (2000) 698–701

PHYSICA E

www.elsevier.nl/locate/physe

# Non-ohmic vertical transport in multilayered quantum hall systems

Minoru Kawamura *, Akira Endo, Shingo Katsumoto [1], Yasuhiro Iye [1]

*Institute for Solid State Physics, University of Tokyo, 7-22-1, Roppongi, Tokyo 106-8666, Japan*

**Abstract**

The vertical transport in weakly coupled multilayered two-dimensional electron systems has been studied in the integer quantum Hall regime. The current–voltage characteristics show prominent non-ohmicity in the vertical transport when each layer is in the quantum Hall state. The voltage dependence curves of the differential conductivity scaled by the mesa perimeter collapse onto a single curve at lower voltages, while those scaled by mesa area are on a single curve at higher voltages. This shows that the current flows through the surface of the sample at low-voltage region and through the bulk at high-voltage region. A crossover from the surface transport to the bulk transport occurs in a fairly narrow range of the bias voltage.


*PACS:* 73.40.Hm; 73.20.Dx

*Keywords:* Vertical transport; Superlattice; Quantum Hall effect; Chiral surface state

Two-dimensional electron gas (2DEG) exhibits the integer quantum Hall effect (QHE) when placed under a strong magnetic field. The issue of the QHE in weakly coupled multilayered 2DEG systems has been addressed theoretically and experimentally since early 1980s [1–4]. Störmer et al. [4] first demonstrated experimentally that the quantized Hall resistance and the vanishing diagonal resistance occur in the presence of the interlayer coupling in semiconductor superlattice. Multilayered quantum Hall systems have recently gained renewed interest by the theoretical prediction [5,6] of the existence of a new metallic state at the periphery of the sample, called a chiral surface state. At the edge of an isolated 2D quantum Hall state, edge channels are formed which are free from backscattering because of their chirality. When interlayer transfer is introduced, the edge states in adjacent 2D planes are coupled to form a metallic 2D sheath at the periphery of the sample. The electrons in a chiral surface state are expected to flow ballisticaly in the in-plane direction and diffusively in the out-of-plane direction. Despite of its 2D character, the surface state is free from the localization (interference) effect because of the chirality along the in-plane direction. This enables us to observe metallic 2D sheet conductivity smaller than $e^2/h$.

The existence of such surface states is confirmed experimentally by Druist et al. [7] They have found that the vertical conductivity in the QHE regime scales with the sample perimeter at low enough temperatures.

* Corresponding author.

[1] Also at CREST, Japan Science and Technology Corporation, Japan.

1386-9477/00/$ - see front matter 
PII: S1386-9477(99)00176-9

At higher temperatures where the current mainly flows through bulk, the vertical conductivity scales with the sample area. In the present work, we have found that the current–voltage characteristics in the QHE regimes exhibits prominent nonlinearity.

Sets of two identical $GaAs/Al_{0.15}Ga_{0.85}As$ superlattice wafers were grown. One wafer for the vertical transport was grown on an $n^+$ GaAs substrate and capped with a heavily doped $n^+$ GaAs layer. The other wafer for the lateral transport was grown on a semi-insulating GaAs substrate. The superlattice part consists of 100 units of 10 nm wide GaAs well layer and 15 nm wide AlGaAs barrier layer. The total height of superlattice is $L = 2.5$ μm. Relatively low Al content $x = 0.15$ was chosen to achieve a sufficient large interlayer transfer integral. Si donors were doped only in the central 5 nm of the AlGaAs barrier layer to a concentration $1.3 \times 10^{18}\,\mathrm{cm}^{-3}$. For the vertical transport, square columnar mesas were fabricated by photolithography and wet chemical etching. Ohmic contact was achieved by standard AuGe alloying technique on the top face of the mesa and the backside of the chip. Four mesas with different crosssections were fabricated on a single chip, $50 \times 50$, $100 \times 100$ and $200 \times 200$ and $400 \times 400$ $\mu m^2$. A schematic picture of the sample for the vertical transport is shown in the inset of Fig. 2(a). The samples for the lateral transport was patterned into the Hall bar shape. Magnetotransport measurements was carried out using a dilution refrigerator down to 30 mK in a superconducting solenoid up to 15 T. A standard AC lock-in technique was employed for the resistance measurement.

Magnetic field dependence of the in-plane resistance $R_{xx}$ and the Hall resistance $R_{xy}$ at 30 mK are shown in Fig. 1(a). From these lateral transport data, we obtain the sheet carrier density $n = 2.3 \times 10^{15}\ \mathrm{m}^{-2}$/layer and the mobility $\mu = 6300\ \mathrm{cm}^2/\mathrm{Vsec}$. The QHE at filling factors $\nu = 1$ and 2 are clearly seen. In Fig. 1(b), the magnetic field dependence of the out-of-plane resistance $R_{zz}$ are plotted for three samples with sizes $50 \times 50, 100 \times 100$ and $200 \times 200$ $\mu m^2$. The $R_{zz}$ curve takes large maxima at magnetic field values where the lateral transport shows the QHE. The inset of Fig. 1(b) shows the size dependence of the out-of-plane conductance $G_{zz} = 1/R_{zz}$ at filling $\nu = 2$. The proportionality of

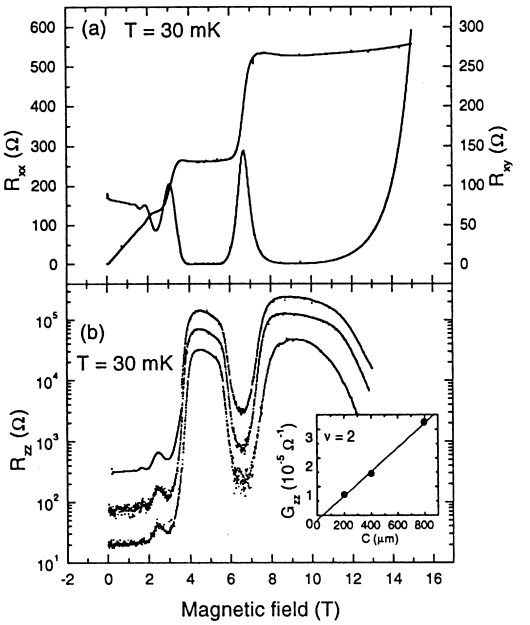


Fig. 1. (a) Magnetic field dependence of the in-plane resistance $R_{xx}$ and the Hall resistance $R_{xy}$; (b) magnetic field dependence of the out-of plane resistance $R_{zz}$ in three samples with cross-sections, $50 \times 50, 100 \times 100$ and $200 \times 200$ $\mu m^2$ (from top to bottom). The inset shows $G_{zz}$ at $\nu = 2$ versus sample perimeter.

$G_{zz}$ to the mesa perimeter indicates that the current is carried by the surface channels.

The temperature dependence of the out-of-plane conductance $G_{zz}$ at $\nu = 2$ is plotted in Fig. 2. The vertical axis is scaled by mesa perimeter in Fig. 2(a) and by mesa area in Fig. 2(b). The out-of-plane conductivity decreases rapidly with decreasing temperature following an Arrhenius-type temperature dependence and tends to an almost constant value below 100 mK. Above 100 mK, the out-of-plane conductivity scaled by mesa area is on a single curve indicating that the transport in the high-temperature region is through the bulk of the sample. On the other hand, below 100 mK, the almost temperature-independent values of the out-of-plane conductivity are scaled by mesa perimeter. This implies that transport is through the surface channels. These results essentially reproduce those reported by Druist et al. [7]. The value of the sheet conductivity $\sigma_{zz}^{2D} = G_{zz}L/C = 2.5 \times 10^{-3} e^2/h$ is on the same order of magnitude as $1.2 \times 10^{-3} e^2/h$ reported in Ref. [7]. According to Balents and Fisher

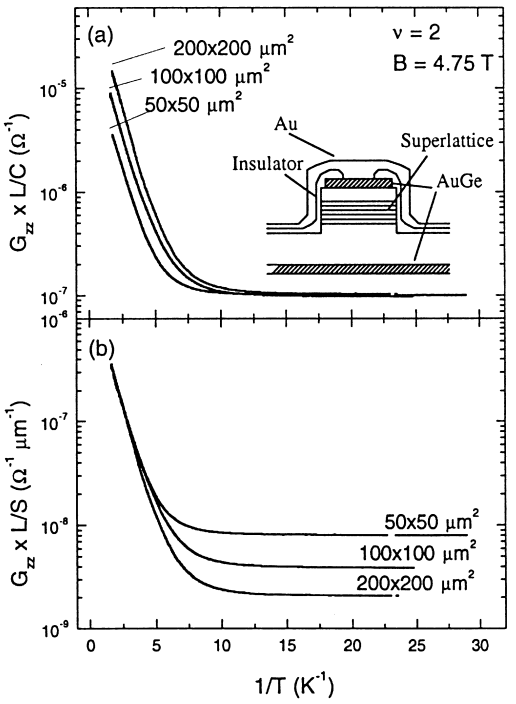


Fig. 2. Temperature dependence of the out-of-plane conductivity $G_{zz}$. The vertical axis is scaled by mesa perimeter in (a) and by mesa area in (b). The inset shows a schematic picture of the sample for the vertical transport.

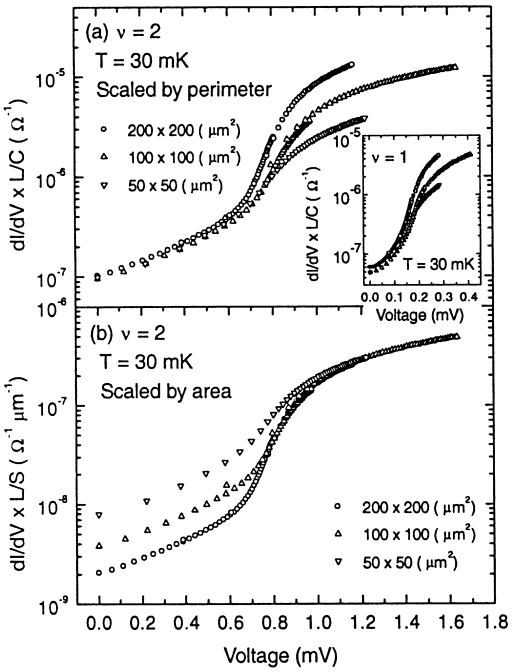


Fig. 3. Voltage dependence of differential conductivity at $\nu = 2$ for three samples with different cross-sections. The vertical axis is scaled (a) by mesa perimeter and (b) by mesa area. The inset shows the similar non-ohmic behavior at $\nu = 1$.

[6], the sheet conductivity of the chiral surface states at filling $\nu = N$ is given by

$$\sigma_{zz}^{2D}(\nu = N) = Ne^2\rho D = N\frac{e^2t^2\tau a}{2\pi\hbar^3 v}, \quad (1)$$

where $\rho = 1/hva$ is the density of state, $D = (ta/\hbar)^2\tau$ is the diffusion constant in the $z$ direction, $t$ is the interlayer transfer integral, $\tau$ is the elastic scattering time, $a$ is the interlayer spacing and $v$ is the electron velocity of the edge state. This formula contains two unknown parameters $\tau$ and $v$ which are difficult to determine independently. This makes it hard to compare the sheet conductivity between different samples, or with the theoretical prediction.

Above 100 mK, the measured conductance $G_{zz}$ shows the Arrhenius-type temperature dependence, $G_{zz} \propto \exp(-E_a/k_BT)$, with the activation energy $E_a = 0.95 \pm 0.05$ K which is much smaller than $\hbar\omega_c/2 = 4.1$ meV $= 48$ K. Note that there is a band of extended states with the bandwidth $4t$ at the center of each Landau subband. Although it decreases the activation energy to $\hbar\omega_c/2 - 2t$, the bandwidth $4t = 0.12$ meV is too small to explain the experimental data. The observed small activation energy implies that the relevant conduction process is not the excitation to the extended states at the center of Landau subbands but the hopping among the localized states. The activation energy for the latter process might be much smaller than $\hbar\omega_c/2 - 2t$, although it is hard to estimate since it depends sensitively on the random potential profile.

Now we turn to the current–voltage ($I$–$V$) characteristics. We measured the out-of-plane differential resistance by varying the applied DC bias current. In Fig. 3, we plot the inverse of the measured differential resistance (i.e. differential conductance) at 30 mK as a function of the voltage across the superlattice part. The vertical axis is scaled by mesa perimeter in Fig. 3(a) and by mesa area in Fig. 3(b) in the same manner as done in Fig. 2. In the low-voltage region, the differential conductance curves scaled by mesa perimeter

collapse onto a single curve, while those by mesa area are on a single curve at higher voltages. As the voltage is increased, a crossover from the surface transport to the bulk transport occurs in a fairly narrow voltage range. Similar non-ohmic behavior is observed at a filling factor $\nu = 1$ as shown in the inset of Fig. 3. The voltage for the crossover from the surface transport to the bulk transport for $\nu = 1$ is smaller than that for $\nu = 2$.

It is also noted that the differential conductance exhibits significant voltage dependence even in the region away from the crossover. The non-ohmicity in the high-voltage region, where the current mainly flows through the bulk, is attributed to the non-linearlity in the hopping process among the localized states near the Fermi level [8]. Non-ohmicity is also observed in the low-voltage region. It is noteworthy that the sheet conductance in this region is almost independent of temperature. This non-Ohmicity, together with the sheet conductivity much smaller than $e^2/h$, reflects the marginally metallic nature of the chiral surface state.

According to the recent theory of Cho et al. [9], transport behavior of the chiral surface state critically depends on the relation between the sample size and the characteristic length scales. Particularly important in the present system is the fact that the de-phasinglength is much shorter than the sample size in both the in-plane and out-of-plane directions. This renders the present system an incoherent 2D chiral metal. Following Ref. [9], the de-phasing length in the in-plane direction is estimated as $l_\phi \sim 20$ μm and the out-of-plane direction $L_\phi = \sqrt{a\sigma l_\phi}$ is on the order of $\sim a$ by using the measured $\sigma = 2.5 \times 10^{-3}(e^2/h)$. This is close to the "sequential tunneling" limit. Since the drift velocity along the $z$-direction is not defined in this limit, we should replace the diffusion constant $D = (ta/\hbar)^2\tau$ in Eq. (1) with $D = a^2/\tilde{\tau}$. Here, $1/\tilde{\tau}$ is the interlayer scattering rate for an electron travelling in the edge channel. The out-of-plane conductivity in the "incoherent" limit is thus $\sigma_{zz} = (e^2/hva) \times a^2/\tilde{\tau}$. In this picture, the non-ohmicity may be attributed to the change in the scattering rate $1/\tilde{\tau}$ with bias voltage. It is, however, not clear whether this line of interpretation is quantitatively reasonable, since the bias voltage per layer unit is on the order of a few microvolts.

## References

[1] M.Ya. Azbel, Phys. Rev. B 26 (1982) 3430.
[2] B.I. Halperin, Jpn. J. Appl. Phys. 26 (Suppl.) (1987) 1913.
[3] T. Ohtsuki et al., J. Phys. Soc. Japan 62 (1993) 224.
[4] H.L. Störmer et al., Phys. Rev. Lett. 56 (1985) 85.
[5] J.T. Chalker, A. Dohmen, Phys. Rev. Lett. 75 (1995) 4496.
[6] L. Balents, M.P.A. Fisher, Phys. Rev. Lett 76 (1996) 2782.
[7] D.P. Druist et al., Phys. Rev. Lett. 80 (1998) 365.
[8] M. Kawamura et al., J. Phys. Soc. Japan 68 (1999) 2186.
[9] S. Cho et al., Phys. Rev. B 56 (1997) 15 814.